Przemysław GORCZYCA*, Maciej ROSÓŁ*

MODELLING OF THE SEMI-ACTIVE SUSPENSION SYSTEM

SUMMARY

The paper is concerned with a mathematical model of the Semi-Active Suspension system (SAS) of a vehicle equipped with the magnetorheological rotary brake manufactured by the Lord Corporation. SAS is a laboratory system animating the suspension action of a car quarter. A simulation model written in the MATLAB/Simulink environment is shown. The parameters of the mathematical model are identified by optimization procedures based on experimental data collected in the real-time. The mathematical model is verified. It means that appropriate system trajectories of SAS and the simulation model are compared.

Keywords*: semi-active suspension, modelling, MR brake, identification*

MODEL PÓŁAKTYWNEGO SYSTEMU ZAWIESZENIA

W pracy przedstawiono model matematyczny półaktywnego systemu zawieszenia (SAS) pojazdu, wyposażonego w obrotowy hamulec magnetoreologiczny wyprodukowany przez firmę Lord Corporation. SAS jest laboratoryjnym systemem animującym działanie zawieszenia ćwiartki pojazdu. Przedstawiony w pracy model symulacyjny został wykonany w środowisku MATLAB/Simulink. Parametry modelu matematycznego zostały wyznaczone przy użyciu procedur optymalizacyjnych wykorzystujących dane zebrane w trakcie prowadzonych w czasie rzeczywistym eksperymentów. Weryfikację modelu matematycznego wykonano, porównując odpowiedzi modelu symulacyjnego oraz obiektu.

Słowa kluczowe*: półaktywne zawieszenie, modelowanie, hamulec magnetoreologiczny, identyfikacja*

1. INTRODUCTION

A number of devices equipped with magnetorheological (MR) dampers, brakes and clutches are manufactured. The main purpose of these devices is to reduce vibrations in real-time operating systems (Gorczyca *et al.* 2009, Rosół and Gorczyca 2009, Sapiński and Bydoń 2004). The other purposes are of the verification of a MR device design (Li and Du 2003), modeling (Jang *et al.*, 2002, Vavreck and Ching-Han 2005), prediction of MR device performance (Bica 2004) etc.

In the paper the SAS system manufactured by the Inteco company in Krakow is examined. SAS is able to animate an action of a car quarter suspension. It contains a rotary MR brake which enables a user to change the suspension parameters.

A simulation model written in the MATLAB/Simulink environment is shown. The model parameters are identified and verified by the SAS real-time experiment. In detail, the RD-2087-01 rotary brake manufactured by the Lord Corporation is examined (Lord Corp. 2006). It is a compact, magnetorheological (MR) fluid proportional brake. As a magnetic field is applied to the MR fluid inside the brake, the viscosity of the fluid is changed to provide increased torque output with practically infinite precision (Vavreck *et al.* 2009). The damping effectiveness is adjusted by varying the brake coil current. The restoring torque in the MR brake depends on the rotational velocity of the brake's axle and the magnetic field strength.

A nonlinear model for the MR brake is considered. The data collected during experiments are used, together with an optimization procedure to determine the model parameters.

2. MODEL OF THE SYSTEM

The mathematical model presented in this section describes a behavior of the laboratory SAS system equipped with a MR rotary brake (Rosół and Gorczyca 2009). The SAS is driven by a DC motor, equipped with a gearbox, coupled to an eccentric small wheel (Fig. 1). The suspended car wheel rolls due to the small wheel rotation and oscillates up and down due to the small wheel eccentricity. A higher angular DC motor velocity results in a higher frequency of the car wheel vertical oscillations. As far as the amplitude of oscillations is concerned one can notice that the maximal magnitude occurs at the natural frequency of the car body. There are two lever angles of the car wheel suspension (unsprung mass) and the car body suspension (sprung mass) and the small eccentric wheel rotational angle (kinematic excitation).

To construct the mathematical model a simple addition of the moments is applied. The mathematical model is developed under some simplifying assumptions:

- dynamics of the SAS can be described by ordinary differential equations,
- friction of the system is viscous type,
- axle of the rotation is common for both arms.

* AGH University of Science and Technology, Faculty of Electrical Engineering, Automatics, Computer Science and Electronics, Department of Automatics, al. A. Mickiewicza 30, 30-059 Krakow, Poland; przemgor@agh.edu.pl; mr@agh.edu.pl

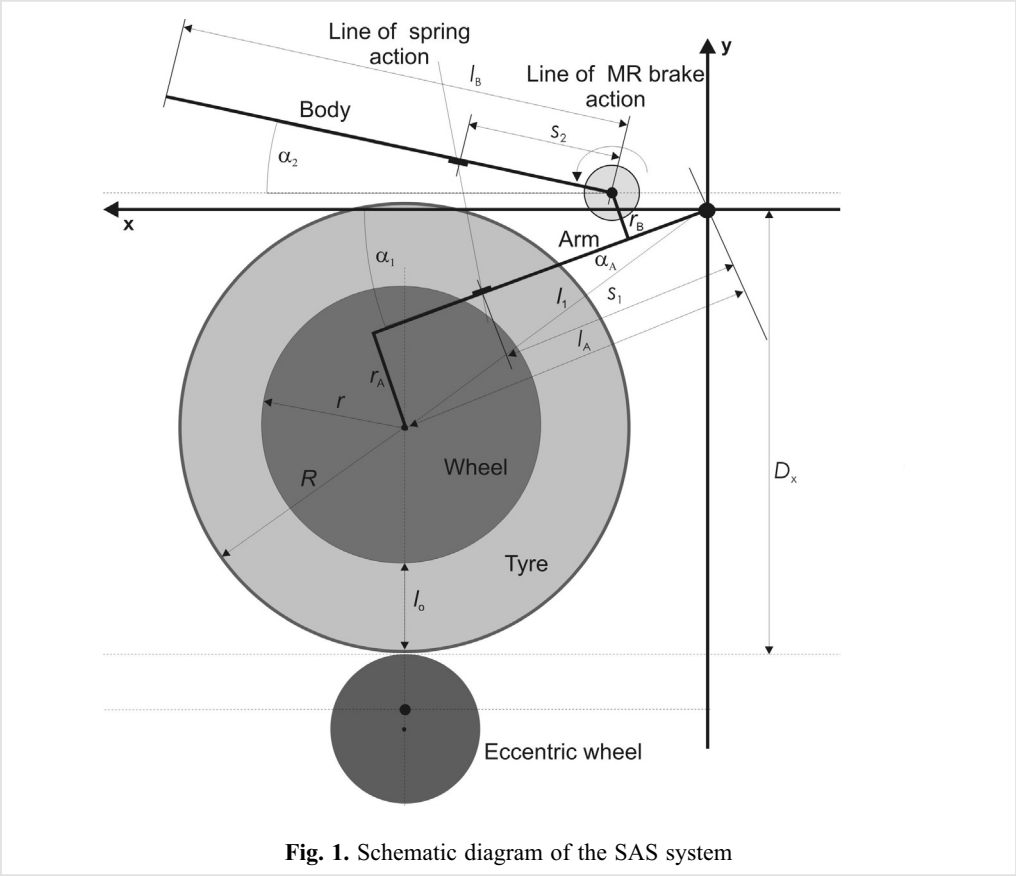

Fig. 1. Schematic diagram of the SAS system

Finally, the mathematical model of the SAS becomes a set of two ordinary second order nonlinear differential equations, being the state equations (1)–(2):

$$J_2\frac{d^2\alpha_2}{dt^2}-k_2\frac{d\alpha_2}{dt}+ \\ +M_2\cos\alpha_2-r_2k_s\left(l_{0s}-\Delta l\right)=T_{MR}(i) \tag{1}$$

$$J_1\frac{d^2\alpha_1}{dt^2}-k_1\frac{d\alpha_1}{dt}+M_1\cos(\beta-\alpha_1)+r_1k_s\left(l_{0s}-\Delta l\right)- \\ -k_gR\cos(\beta-\alpha_1)\left[l_{0g}+R\sin(\beta-\alpha_1)+r-D_x+u_{kin}\right]- \\ -f_g\left[\frac{d(D_x-u_{kin})}{dt}-\frac{d\alpha_1}{dt}R(\beta-\alpha_1)\right]=T_{MR}(i) \tag{2}$$

where:

$$\Delta l=\sqrt{(r_2\cos\alpha_2-r_1\sin\alpha_1)^2+(r_2\sin\alpha_2-r_1\cos\alpha_1)^2}= \\ =\sqrt{r_1^2+r_2^2-2r_1r_2\sin(\alpha_1+\alpha_2)},$$

$$T_{MR}(i)=T_{rd}(i)+k_{rd}(i)\left(\frac{d\alpha_1}{dt}-\frac{d\alpha_2}{dt}\right),$$

α_1 – angle between the wheel arm and the horizontal line,
α_2 – angle between the body car and the horizontal line,
β – angle between lower beam and the horizontal line,
r – radius of the wheel rim,
r_1, r_2 – distances between the spring mount and the beam (the lower and upper),
l_{0s} – length of the no-load spring,
l_{0g} – length of the loaded spring,
R – distance between the beam pivots,
D_x – distance between the beam pivot and the pivot of the eccentric wheel,
J_1 – moment of inertia of the lower beam with respect to its axis of rotation,
J_2 – moment of inertia of the upper beam with respect to its axis of rotation,
M_1 – gravitational moment of the lower beam,
M_2 – gravitational moment of the upper beam,
k_1 – viscous friction coefficient of the lower beam,
k_2 – viscous friction coefficient of the upper beam,
k_s – elasticity coefficient of the spring,
k_g – elasticity coefficient of the tire,
f_g – absorption coefficient of the tire,
u_{kin} – control signal of the kinematic excitation,
i – current in the MR brake
$T_{MR}(i)$ – torque of the MR brake,
$T_{rd}(i)$ – static profile of the MR brake torque,
$k_{rd}(i)$ – static profile of the MR brake viscous friction coefficient.

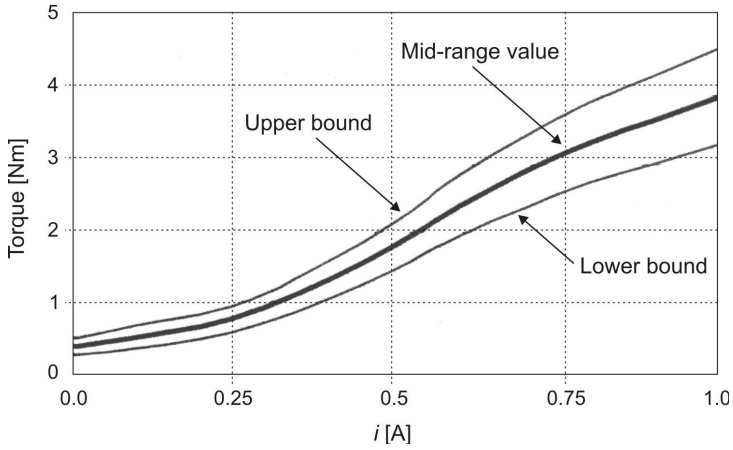

Fig. 2. Torque curve for the Lord RD-2087-01 (Lord Corp. 2006)

Initial conditions for equations (1) and (2) are set to $\alpha_{10}, \alpha_{20}, \frac{d\alpha_1}{dt} = 0, \frac{d\alpha_2}{dt} = 0.$

The plot of the MR brake torque vs. coil current is shown in Figure 2. One can notice that the hysteresis is not involved in the model. Therefore, this approach is simplified as far as more complex models are concerned, for example the Bingham and the Bouc-Wen models. The idea to use the simplified model is justified. Since the models for control do not need to be very complex.

3. MODEL IDENTIFICATION AND VERIFICATION

The parameters of the mathematical model (1) are identified by using an optimization procedures based on collected experimental data. Experiments are conducted at the laboratory rig shown in Figure 3. The block diagram of the rig comprises the SAS laboratory model, power interface, PC working under Windows 7 equipped with RT-DAC/USB 2.0 board. Two lever angles of the car wheel and the car body and rotational angle of the eccentric wheel are measured with the incremental encoder sensors HEDM-5055 (4096 pulses per revolution).

The primary experiment is performed to identify the parameters of the MR rotary brake, the elasticity coefficient of the spring, the moment of inertia of the upper beam and the viscous friction coefficient of the upper beam. These experiments are performed for a simplified structure of the SAS upper part presented schematically in Figure 4.

The car body position is disturbed manually to abandon the steady-state position. Then it begins to vibrate and a free motion of the car body for various currents of the MR rotary brake coil can be observed. The frequency of the oscillations which in fact is the resonant frequency of the system is equal to 1.46 Hz.

The optimization procedure *fminsearch* from MATLAB Optimization Toolbox is used. The optimization results confirm that the T_{rd} and k_{rd} of the MR rotary brake are the nonlinear functions of the applied coil current. The relation between the MR brake torque, the MR brake viscous friction coefficient and the current is illustrated in Figures 5 and 6 respectively. The identified $T_{rd}(i)$ curve is similar to the one presented by the manufacturer in Figure 2.

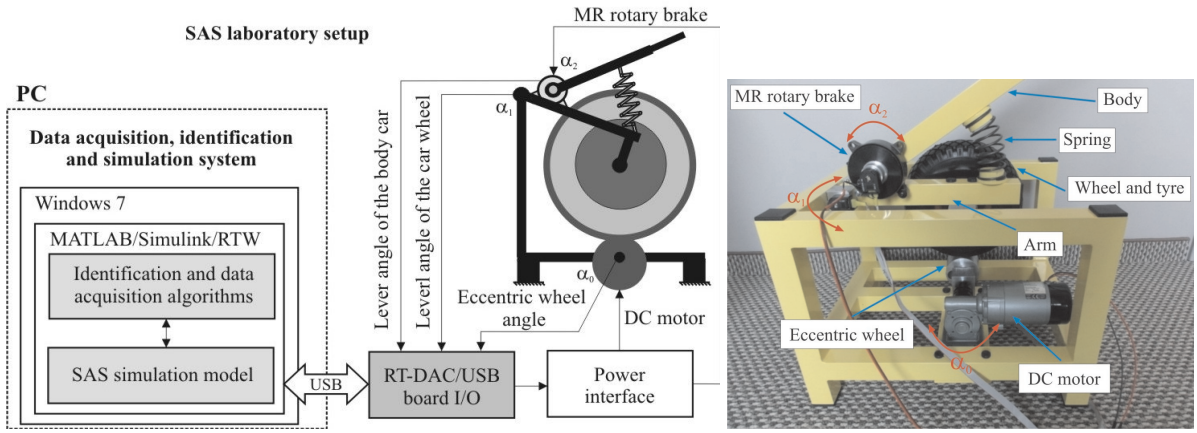

Fig. 3. Block diagram of the experimental setup and a general view of the SAS

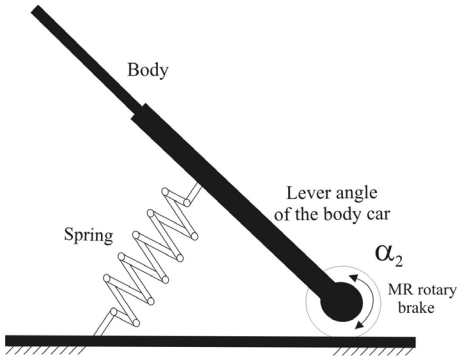

Fig. 4. Structure of the body suspension

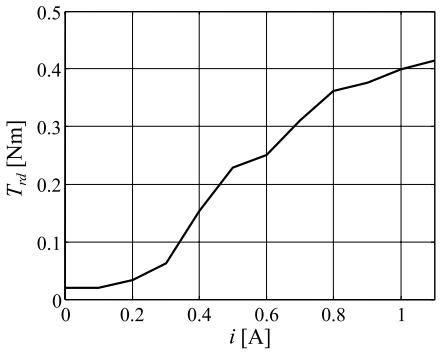

Fig. 5. The MR brake torque vs. current

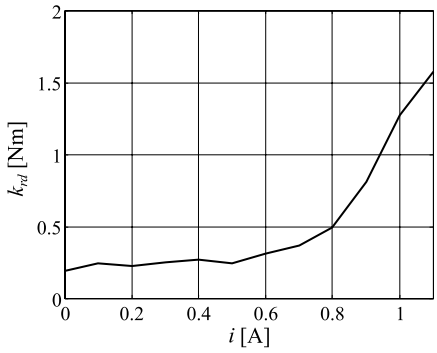

Fig. 6. The MR brake viscous friction coefficient vs. current

The Figure 7 compares the body car angle obtained from the experiments and simulation model collected for two values of the MR brake coil: $I_1 = 0.5$ A and $I_2 = 1.0$ A. As far as large amplitudes are concerned the model parameters fits quite accurately in contrast to small amplitude then the friction phenomena introduced discrepancies in the model. As can be noticed the number of vibration cycles decreases when the current value increases (Rosół and Gorczyca 2009).

At the next identification step the following SAS parameters are fixed: (J_2, k_2, M_2, k_s, k_2, T_{rd}, k_{rd}). The other SAS parameters: (J_1, k_1, M_1, k_g, f_g) are calculated using the same *fminsearch* procedure.

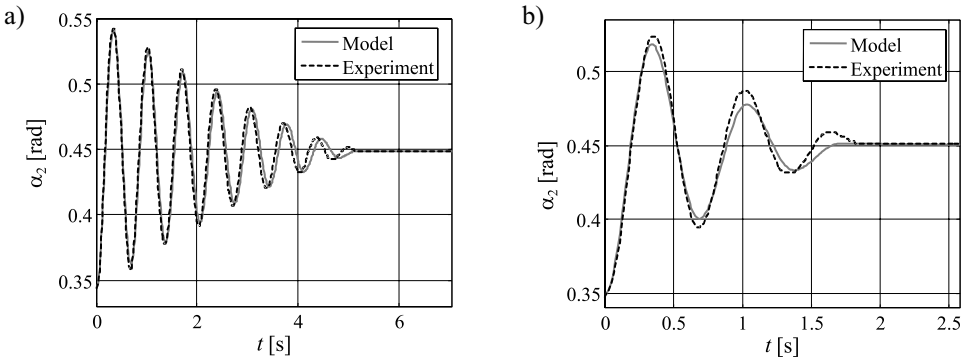

Fig. 7. Time pattern of the body car angle: a) $I_1 = 0.5$ A; b) $I_2 = 1.0$ A

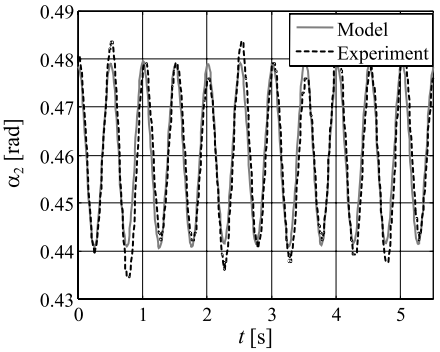

Fig. 8. Time pattern of the α_2 for $I_1 = 0.5$ A

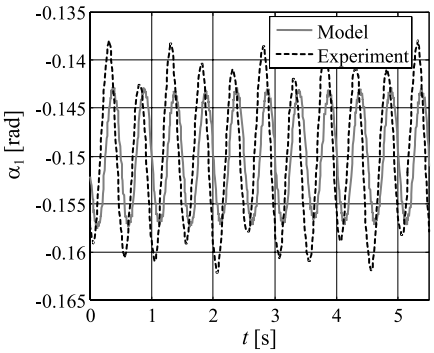

Fig. 9. Time pattern of the α_1 $I_1 = 0.5$ A

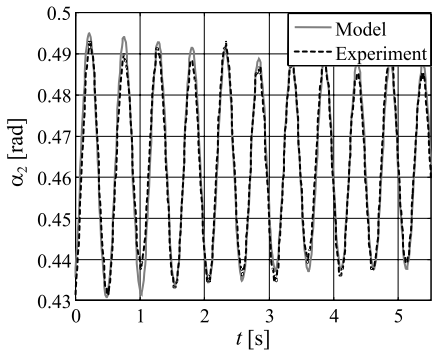

Fig. 10. Time pattern of the α_2 for $I_2 = 1.0$ A

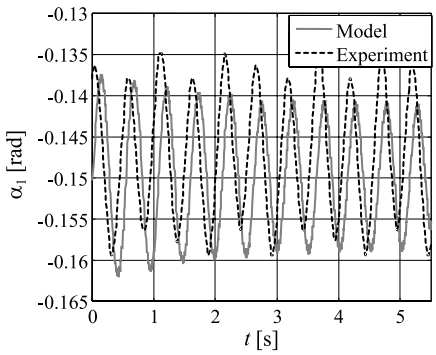

Fig. 11. Time pattern of the α_1 for $I_2 = 1.0$ A

In order to conduct the experiments the excitation signals are defined. Their amplitude is ±0.05 m in the frequency range (0.5–8) Hz. Selected results of optimization are shown in Figures 8–11, which compare the measured body car and wheel car angles with these obtained from the simulation model (sine excitations at frequency equal to 2.0 Hz). Figures 8 and 9 present results for $I_1 = 0.5$ A, while Figures 10 and 11 for $I_2 = 1.0$ A.

The α_1 and α_2 angle magnitudes and shapes are similar among the experimental data and model responses. However, the small phase shift of the α_1 angle can be observed (Fig. 11).

The all geometrical and identified parameters of the mathematical model are collected in the Table 1.

4. SUMMARY

The mathematical model of the SAS system including a simple nonlinear model of the MR rotary brake is presented. The parameters of the SAS model are identified by using the parametric optimization procedures. The optimization is performed using input time series data of the body and wheel car positions in a long amount of time (30 seconds) to obtain the seven parameters of the SAS model (k_1, k_2, J_1, J_2, k_g, f_g, k_s) and MR brake characteristics.

The mathematical model has been verified. It means that the real and simulated trajectories were compared. The coefficients as well as the structure of model are settled.

Table 1

Parameters of the SAS mathematical model

Parameter		Value
Geometrical	R [m]	0.225
	r [m]	0.066
	r_1 [m]	0.226
	r_2 [m]	0.92
	l_{0s} [m]	0.179
	l_{0g} [m]	0.103
	D_x [m]	0.2
	β [rad]	0.172
Lower part of the SAS	J_1 [kg·m^2]	3.68
	M_1 [N·m]	4.5368
	k_1 [N·m·s/rad]	1.0245
	k_g [N/m]	3846.3
	f_g [N·s/rad^2]	141.1
Upper part of the SAS	J_2 [kg·m^2]	0.71
	M_2 [N·m]	1.12
	k_2 [N·m·s/rad]	0.682
	k_s [N/m]	2827

However, a number of additional experiments would be necessary to enhance the SAS dynamical model. The simplified MR model is not sufficient. A special laboratory set – the micro engine test house – will be constructed to de-velop a braking moment model dependent on the current and rotary speed.

Acknowledgement

This paper was supported by the research grant of the AGH University of Science and Technology No. 11.11.120.768.

References

Bica I. 2004, *Magnetorheological Suspension Electromagnetic Brake*. Journal of Magnetism and Magnetic Materials, vol. 270, No. 3, April, pp. 321–326.

Gorczyca P., Kołek K., Rosół M., Turnau A. 2009, *Semi-active Suspension Laboratory System*. Solid State Phenomena vols. 147–149, Trans. Tech. Publications, Switzerland, pp. 350–355.

Li W.H., Du H. 2003, *Design and Experimental Evaluation of a Magnetorheological Brake*, International Journal of Advanced Manufacturing Technology, vol. 21, No. 7, pp. 508–515.

Lord Corporation 2006, *RD-2087-01 Rotary Brake. Technical data*. http://www.lord.com.

Rosół M., Gorczyca P. 2009, *Semi-active suspension system with an MR rotary damper*. Mechanics (AGH University of Science and Technology), vol. 28, No. 2, pp. 60–64.

Sapiński B., Bydoń S. 2004, *Characteristics for a magnetorheological rotary brake – experimental investigation*. Proc. of Int. Carpathian Control Conf., pp. 373–378.

Vavreck A.N., Ching-Han Ho 2005, *Characterization of a commercial magnetorheological brake/damper in oscillatory motion*. Smart Structures and Materials 2005: Damping and Isolation, edited by Kon-Well Wang, Proc. of SPIE, vol. 5760.

Yang G., Spencer B.F., Jr., Carlson J.D., Sain M.K. 2002, *Large-Scale MR Fluid Dampers: Modeling and Dynamic Performance Considerations*. Engineering Structures, vol. 24, No. 3, March, pp. 309–323.